Reactive self-tracking solar concentrators: concept, design, and initial materials characterization

Katherine A. Baker,[1,*] Jason H. Karp,[1,2] Eric J. Tremblay,[1,3] Justin M. Hallas,[1,4] and Joseph E. Ford[1]

[1]Department of Electrical and Computer Engineering, University of California, San Diego, 9500 Gilman Drive, Mail code 0409, La Jolla, California 92093, USA

[2]General Electric Global Research, Niskayuna, New York 12309, USA

[3]École Polytechnique Fédérale de Lausanne, Lausanne, Switzerland

[4]Pacific Integrated Energy, San Diego, California 92130, USA

*Corresponding author: kabaker@ucsd.edu

Received 28 September 2011; accepted 1 November 2011; posted 18 November 2011 (Doc. ID 155228); published 6 March 2012

Étendue limits angular acceptance of high-concentration photovoltaic systems and imposes precise two-axis mechanical tracking. We show how a planar micro-optic solar concentrator incorporating a waveguide cladding with a nonlinear optical response to sunlight can reduce mechanical tracking requirements. Optical system designs quantify the required response: a large, slow, and localized increase in index of refraction. We describe one candidate materials system: a suspension of high-index particles in a low-index fluid combined with a localized space-charge field to increase particle density and average index. Preliminary experiments demonstrate an index change of aqueous polystyrene nanoparticles in response to a low voltage signal and imply larger responses with optimized nanofluidic materials. © 2012 Optical Society of America

OCIS codes: 350.6050, 220.1770, 160.4236.

1. Introduction

In concentrator photovoltaic (CPV) modules, large collection area optics focus sunlight onto small area photovoltaic cells, making it cost effective to use efficient (record 43.5%) but expensive ($5–10/cm^2) multijunction cells [1–3]. While low concentration (~10×) CPV systems can be passive, high-concentration (~100–1000×) systems require accurate two-axis mechanical tracking to maintain solar alignment, due to low angular acceptance. This tracking is an integral part of existing CPV systems since expanding the angle of accepted beams by modifying the optical system necessarily reduces the potential concentration of the system. Angular limitation of the entrance and exit apertures are related to geometric concentration through the principle of étendue, which states that the product of the aperture size and acceptance angle is equal for both entrance and exit. Thus, for a high concentrator optic where the exit aperture is much smaller than the input aperture, the entrance acceptance angle must be much less than the output emission angle. For a system where the input and output beams are in the same medium, the maximum 3D concentration $C_{\max}$ is fundamentally limited by Eq. (1) where θ is the entrance half-angle [4]:

$$C_{\max} = \left(\frac{1}{\sin\theta}\right)^2. \quad (1)$$

Weber and Lambe proposed a different approach to circumvent étendue limits and achieve high

1559-128X/12/081086-09$15.00/0

concentration without mechanical tracking by using a nonlinear materials response to sunlight [5]. In luminescent solar concentrators (LSC), molecules distributed in an isotropic slab waveguide absorb incoming sunlight incident from any direction, then reemit at a longer wavelength. Most of the reemitted light can be guided to reach the PV device at the edge of the slab, with a geometric concentration equal to the ratio of the input to edge face area. The physical structure is ideal: a thin, inexpensive, and lightweight sheet with a large surface area to capture incident sunlight. It can even be conformal to a supporting surface, provided the curvature is sufficiently low. LSC systems are a topic of ongoing materials research and show great long-term promise [6,7]. In practice, there are many sources of loss within LSC systems, including the initial mode conversion loss, reabsorption of the guided light, and the intrinsic wavelength up-conversion loss. Experimental LSC demonstrations have so far shown low effective concentration (optical efficiency times geometric concentration), and so a concentrator that combines the nontracking physical format of an LSC concentrator with the efficiency of conventional concentrator optics has yet to be identified.

The planar micro-optic waveguide concentrator shown in Fig. 1 is an alternative approach

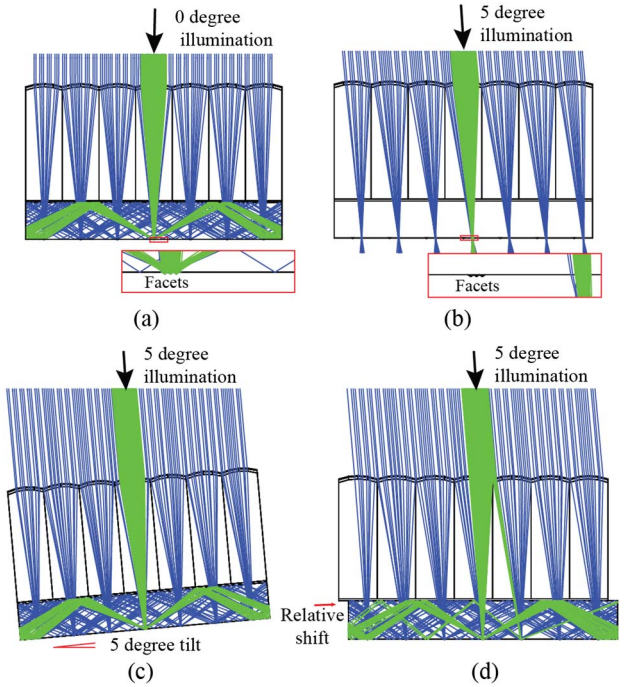

Fig. 1. (Color online) Passive planar micro-optic solar concentrator, showing how normally incident light (a) is coupled into the waveguide by reflection from small facets, while angled light (b) is transmitted through the system and lost. The coupling features are shown in inserts for both the aligned and misaligned systems. A micro-optic solar concentrator can be conventionally aligned by simply tilting the overall structure to restore normal illumination (c), but can also be aligned without bulk mechanical motion via "microtracking" (d) using a small lateral motion of the lenslet relative to the waveguide and coupling features.

to waveguide-based solar concentration [8]. An array of lenslets focuses incoming sunlight through the waveguide and onto small reflective facets, which deflect the light into the waveguide. The coupled light is then directed to high-efficiency multijunction photovoltaic cells at the end(s) of the waveguide. The input coupling facets can also deflect guided light out of the waveguide, which limits the maximum practical concentration and overall efficiency. Optical designs indicate that 300× concentration is achievable with 82% optical efficiency using the basic geometry, increasing to 85% optical efficiency for a 900× concentrator by including additional concentration along the waveguide width and/or incorporating secondary optics between the slab and solar output [9]. This structure offers the potential to reduce the cost of concentrator optics, as the lenslets and waveguide features can potentially be embossed onto glass or plastic sheets using continuous roll processing [10,11]. Other waveguide concentrators have also been demonstrated using planar [12] or stepped [13,14] waveguide structures. Unlike the LSC, these are all passive optical systems. They must obey (at least) étendue limits on solar concentration and alignment to the incident sunlight. Figure 1(b) illustrates the effect of misalignment in a passive micro-optic waveguide concentrator. When the incident light is sufficiently tilted, the focal spots miss the injection facets, and are transmitted rather than coupled into the waveguide. The overall system design is a trade-off: larger coupling features increase waveguide losses but improve tolerance to misalignment.

The waveguide concentrator can be aligned by conventional tracking, tilting the entire structure to maintain normal incidence [Fig. 1(c)]. Another option is to track without bulk mechanical motion of the overall concentrator structure. As Fig. 1(d) shows, a small lateral motion of the waveguide relative to the lenslet array can bring the injection facets into alignment with the current position of the focal spots. Such "microtracking" requires relative positioning to within a fraction of the injection facet diameter. Since the total range of motion is limited to the lenslet pitch, a short-throw precision actuator can provide wide-angle tracking [15,16]. This approach may prove advantageous over two-axis tracking concentrators, but any mechanically tracked system still imposes complexity in feedback and actuation.

Here we propose a new approach to tracking, "reactive" solar concentration, which can potentially combine the tracking-free operation of a LSC with the concentration and efficiency of a passive waveguide concentrator (using reflective and refractive micro-optics). If the coupling features in the micro-optic waveguide concentrator are either created or revealed in response to the focused energy of the incident sunlight, then the overall system can use a nonlinear response to achieve automatic alignment to direct sunlight. The nonlinear effect can be a change in the index of refraction or other first-order

properties of the micro-optic structure. This process can be slow and initiated by a small fraction of the incident energy, and so does not necessarily introduce a significant intrinsic loss. Figure 2 shows how the passive micro-optic waveguide concentrator can be modified to use this effect. Now the reflective waveguide injection features extend over the entire lower surface below the waveguide but are separated from the waveguide by a thin layer of low-index cladding material. If the cladding material were a uniform low refractive index, incident light would reflect from the injection features to the right or left but would not couple into waveguided modes and so would be emitted from the waveguide face. If instead of a uniform refractive index, the cladding material responds to the focused spot of incident sunlight by locally increasing its index of refraction to closely match the index of the waveguide, light would not be refracted by the waveguide-cladding interface, and so the reflected light would couple into guided modes. Regions that are not illuminated by focused sunlight maintain a low index and act as a conventional waveguide cladding, so the guided light will propagate with low loss to the waveguide edge. The basic concept of a reactive solar system has recently been proposed for a skylight that transmits only diffuse sunlight and couples direct light into a PV using temperature-induced scattering from a polymer [17].

In Section 2, we show an overall optical design to evaluate the needed materials response and potential performance of one reactive concentrator embodiment. In Section 3, we discuss a specific reactive materials system combining a suspension of high-index nanoparticles in low-index fluid with a weak photovoltaic layer. In Section 4, we present initial materials characterization results for polystyrene nanoparticles in water responding to applied AC voltages. Section 5 provides a summary and conclusion.

2. Reactive Concentrator Design

The geometry of the injection facets imposes a limitation on coupling efficiency over a wide angular range.

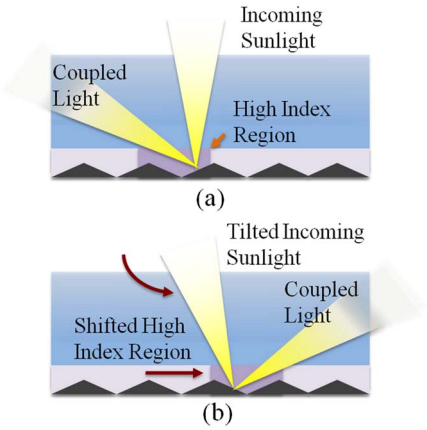

Fig. 2. (Color online) "Reactive-tracking" where the cladding material creates or reveals the coupling features in response to moving focused sunlight.

Incoming sunlight is deflected by 120° angled mirrored prisms. Figure 3 shows how light entering the system from extreme angles is deflected at an angle unable to couple into the slab. The orientation of the tilted coupling facets causes the asymmetry. Light will couple into the waveguide for a much larger change in incoming angle along the length of the prism than along the pitch of the prism. Light tilted at more than 40° along the pitch will not couple.

Implementation of a reactive-tracking system requires lenslets capable of forming a focus over the angular range that can support coupling. Zemax simulations used a 1 mm diameter, 3 mm thick plano-convex singlet lens above a 1 mm F2 glass waveguide and allowed the high-index coupler position to vary with the angular input [Fig. 4(a)]. While a simple singlet lens is suitable for low cost fabrication by continuous roll processing, the focused spot size increases significantly with off-axis illumination due to spherical aberration, coma, and field curvature. Large spot sizes require large high-index regions, leading to coupling loss. A more complex multi-element lenslets can improve resolution at higher angles, though it is constrained by the optical fill factor of the front aperture and wide angle vignetting from

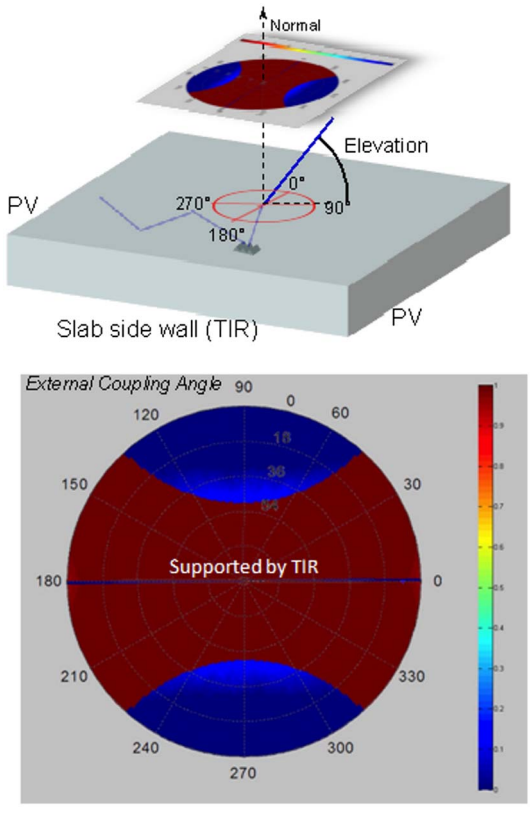

Fig. 3. (Color online) Optical coupling of light reflected from a 120° angled injection facet as a function of external incidence angle (including surface refraction, but not lens effects) for an F2 ($n = 1.62$) waveguide with an air cladding. The vertical-horizontal coupling asymmetry seen in the lower graph results from light reflecting from the adjacent facet and emitting from the entrance aperture.

internal apertures, as well as by the cost of fabrication. Figure 4(b) shows a two-element stack of aspheric singlet lenses: a plano-convex acrylic lens over a plano-concave polycarbonate lens. This lens system can implement smaller high-index regions, leading to reduced overall coupling loss. All surfaces were modeled assuming a simple single layer antireflective coating to limit reflective losses to 0.5%, and all mirrors are ideal silver with an approximate reflectivity of 98%. Cost is a major factor in practical systems, so less expensive, lower performing coatings may need to be used. As shown in Fig. 5(a), the singlet lens can maintain over 80% or higher overall optical efficiency only up to 85× geometric concentration, while the more complex lens can provide 89% efficiency at 85× geometric concentration, and over 80% efficiency up to 230×. For example, a 128× system has 86% performance on-axis, giving it 110× effective concentration on-axis. It may be possible to implement secondary concentration as shown in earlier work to improve the concentration ratio without loss of optical efficiency [9]. At low concentrations, losses in both systems asymptotically approach the fixed 5% loss from surface reflections and mirror absorption. In practice, the achievable fixed surface reflection losses will be affected by manufacturing costs.

These simulations assume that the reactive material begins with a uniform base index and provides a large index change in response to the focal spot. Figure 5(b) shows the dependence of optical system efficiency on both the base and elevated index. In order to achieve the calculated efficiency, the index at the focal spot needed to be more than 0.3 higher than the surrounding bulk fluid, and this was true for a varying base index. However, if the reactive index increases too far over the waveguide index, the reflected light will totally internally reflect within the reactive index volume, strike an adjacent coupling facet, and decouple immediately. The minimal change in index of refraction for optimal efficiency for this system is ~0.3. For example, a system with a base index of 1.25 shows peak efficiency for a high-index spot of 1.55 to 1.75. The wavelength dependence of refractive index could alter this requirement somewhat once real materials are implemented in the design. Lenslets with a larger f-number and a correspondingly smaller cone of light would require a smaller change in index of refraction as the widest angle of the injected light will reach the critical angle sooner, but such a change in f-number will also reduce off-axis performance of the system. This design is a compromise between required index change and off-axis performance.

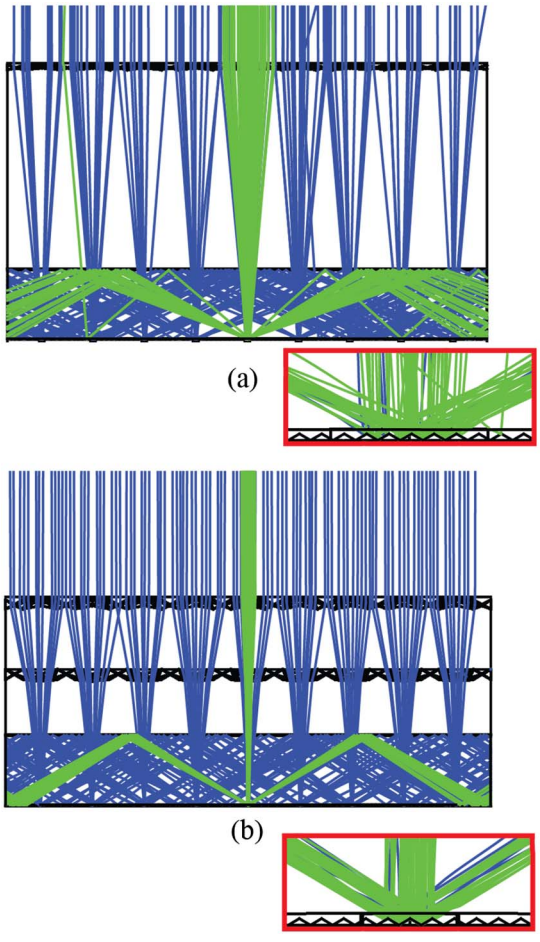

Fig. 4. (Color online) (a) Acrylic singlet lenslet system and (b) acrylic and polycarbonate doublet system with reactive material layer implemented before the coupling facets.

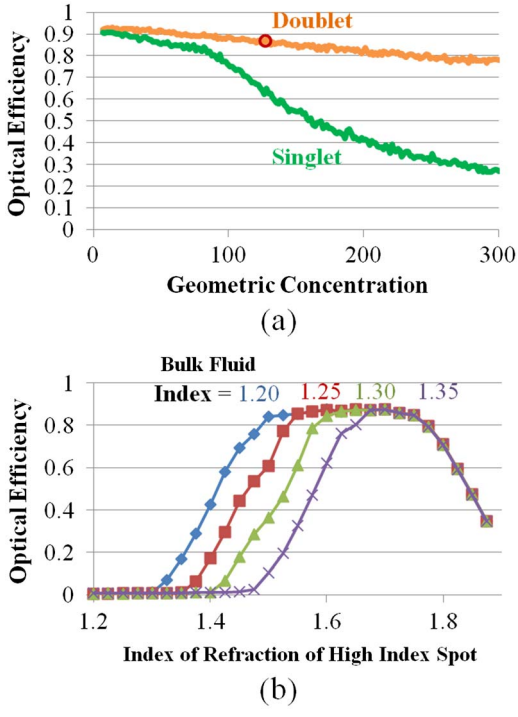

Fig. 5. (Color online) (a) Modeled overall optical system efficiency as a function of geometric concentration ratio for both doublet and singlet lens systems. The model used a 1.25 bulk fluid index and 1.6 index at the focal spot. (b) Modeled optical system efficiency as a function of localized index change for the doublet lens system with 128× geometric concentration (the case indicated by the circled point in the graph above).

To understand the angular acceptance necessary for a practical solar concentrator, Figs. 6(a) and 6(b) show the angular range and intensity of sunlight incident on a static flat panel oriented at latitude for a location at 32.7°, as would be the case for a well-installed passive solar panel in San Diego, California [calculations based on 18]. The reduction in intensity at large angles includes both atmospheric absorption and the relative panel aperture reduction due to tilt. In many commercial solar power applications, direct insolation panels are mounted on 1-axis mechanical tracking concentrators; the 2.4× increase in total incident power gained by eliminating the cosine θ losses more than offsets the cost of the low-precision tracking mechanics, which are far lower than the 2-axis tracking used in CPV systems. The incident solar intensity distribution is shown in Figs. 6(c) and 6(d), which radically changes the input angle requirements. Therefore a practical alternate approach is to use approximate one-axis mechanical tracking with the panel tilted at latitude, and use the reactive concentrator to compensate for seasonal elevation angle changes as well as fine corrections to the azimuthal (East-West) angle. The panel tracks the sun from East to West, but the incoming sunlight will strike the panel at ±23.5 degrees off-axis in the North/South direction.

Figure 7 shows the overall optical concentrator system efficiency as a function of solar incidence angle for the nonreactive prototype, the acrylic singlet system, and the acrylic and polycarbonate doublet system. The lenslets are rotationally symmetric,

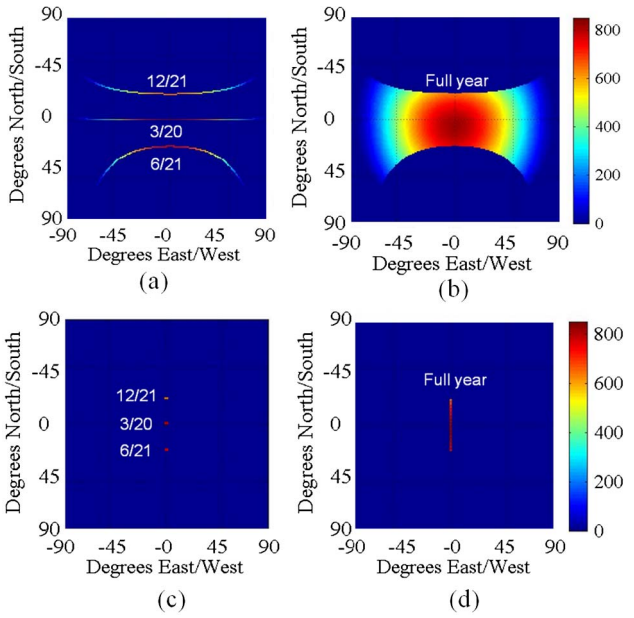

Fig. 6. (Color online) Incident peak sunlight intensity in W/m^2 shown over (a) three key dates and (b) the course of a year relative to a fixed due south flat panel solar collector tilted at latitude in San Diego, California. The intensity roll-off shown is calculated including both air-mass path absorption and cos(θ) loss from the constant aperture orientation. The same data is shown for a 1-axis mechanically tracked panel tilted at latitude in (c) and (d).

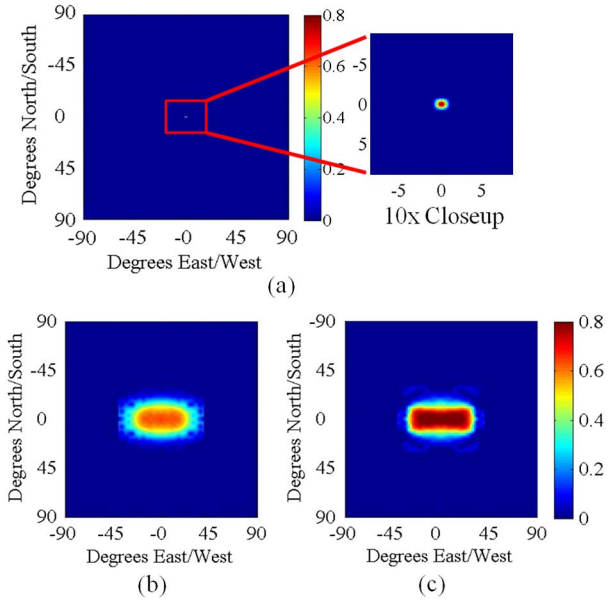

Fig. 7. (Color online) Modeled optical efficiency as a function of input angle for 128× geometric planar solar concentrators with (a) the nonreactive prototype, (b) a reactive singlet lens design, and (c) a reactive doublet lens design. The reactive designs show a substantial increase in angular acceptance over the passive design, which has the low acceptance characteristic of CPV systems.

but the coupling efficiency of the injection facets selectively reduces performance along the axis aligned with the direction of corrugation. Integrating the product of the annual incident energy with the optical efficiency of the reactive concentrator optics results in 25% accepted energy annually for the singlet design and 28% for the doublet. This efficiency would be insufficient for most applications, indicating that a different optical geometry will be needed for a practical fully stationary reactive concentrator. Using the 1D tracking geometry, the singlet reactive concentrator can now capture 60%, and the doublet reactive concentrator can capture 83%, of the annual incident energy, including reflection and absorption losses. With 128× geometric concentration, this represents an efficient relatively high-concentration system without precision tracking.

3. Reactive Materials

Simulations have shown that using a reactive layer in a planar solar concentrator can create a self-tracking system, efficient for at least the range of angles needed for making a high-concentration system combined with 1D mechanical tracking, provided the reactive materials with the necessary index response properties are available. For the incident light on a static collector, the maximum angular velocity of the sun varies with location, and is just less than 0.8 degrees per minute for San Diego. With a 4 mm thick optical system, the focused sunlight on the injection features will move at a maximum of about 40 um per minute within the glass, and much less for most of the day. The response time needed in a 1D tracking system is significantly longer.

One potential materials system to enable the 0.3 (approximately 20%) change in index is a microfluidic system based on localized concentration of high-index nanoparticles suspended in a low-index fluid through optical trapping. Regions of high particle concentration have an average refractive index much higher than regions of low particle concentration. Concentration could be accomplished through optical trapping, which occurs when light passes through a high-index particle and is deflected by refraction. Conservation of momentum causes the particle to move the opposite direction. Particles are drawn closer to the center of the beam by the optical trapping force F_{trap}, which is governed by Eq. (2), where a is the radius of the particle, c is the speed of light, I is the optical intensity, and m is the ratio of the refractive index of the particle to the medium [19]:

$$F_{\text{trap}} = \frac{2\pi a^3}{c}\left(\frac{m^2-1}{m^2+2}\right)\nabla_{\perp} I. \tag{2}$$

As the concentration of particles increases, the average index of refraction increases, changing the dispersion of the light. This effect has been used to generate spatial solitons by passing a high-energy laser beam through a colloidal suspension. If the power of the laser is perfectly matched to the material properties of the colloid, dispersion will be exactly canceled out, creating a soliton [20]. The principal force opposing the trapping force is diffusion, and the subsequent particle flux is given by Eq. (3), where D is the diffusion constant, ν is the mobility D/kT, k is the Boltzmann constant, and T is the temperature. F is the sum of external forces, which for this case is optical trapping. The total concentration is given by Eq. (4) [21]:

$$\vec{j} = -D\vec{\nabla}C + \nu\vec{F}C \tag{3}$$

$$C = C_0 \exp\left(\frac{I}{I_0}\right), \qquad I_0 = \frac{ckT}{2\pi a^3}\frac{m^2+2}{m^2-1}. \tag{4}$$

The Bruggeman model is typically used to calculate index of refraction for high particle concentrations [Eq. (5)], where C is the particle concentration by volume, ε is the overall permittivity of the suspension, ε_2 is the permittivity of the liquid medium, and ε_1 is the permittivity of the particle [22]:

$$C\frac{\varepsilon_2-\varepsilon}{\varepsilon_2+2\varepsilon} + (1-C)\frac{\varepsilon_1-\varepsilon}{\varepsilon_1+2\varepsilon} = 0. \tag{5}$$

The index response could be directly induced in an isotropic colloidal suspension by the electromagnetic properties of light (an incoherent version of laser trapping). The resulting reactive-tracking system is shown in Fig. 8. A sufficiently bright focused spot of sunlight will act as an optical trap for particles, while the diffuse sunlight coupled in the waveguide will not induce trapping (as long as the flux has been sufficiently reduced). This is an elegant approach, but initial calculations indicate it will not generate the index response requirement presented in Section 2. The system is limited by the intensity gradient that can be created from geometric concentration of sunlight, achieved in this case by a relatively small aperture lenslet. Since the trapping force is a function of particle volume, larger particles are needed to create a larger change in index, as shown by Fig. 9, which combines Eqs. (4) and (5) for varying particle size. Even with ideal materials, the 400–600 nm particles needed to obtain necessary change in concentration would cause Mie scattering and also make a stable suspension difficult to achieve. Additional forces such as particle-particle interactions and temperature effects can affect this model, further reducing the index change in a given material [23].

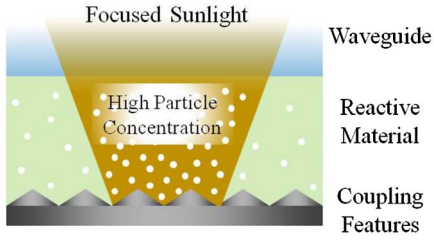

Fig. 8. (Color online) Optical trapping configuration: the focused sunlight traps high-index particles, locally increasing the average index of refraction of the colloid.

Optically induced dielectrophoresis (DEP) provides a mechanism to induce a stronger response in particle trapping. DEP is the movement of neutral particles in a nonuniform electric field, given by Eq. (6), where E_0 is the electric field [24,25]. K, the Clausius-Mosotti factor, is frequency-dependent and can be positive or negative, indicating that particles are attracted to or repelled from the region of highest electric field. Most DEP trapping work uses AC electric fields to take advantage of frequency-dependent effects. However, DEP occurs in nonuniform DC electric fields and existing work has used DC DEP [26]:

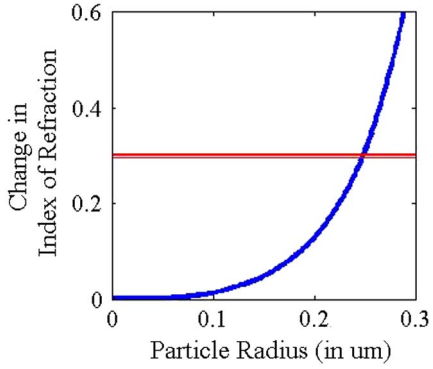

Fig. 9. (Color online) Modeling of maximum index change as a function of particle radius for a 1 mm paraxial lens focusing solar spectrum light to a 4.5 um spot, assuming titanium dioxide suspended in perfluorotriamylamine solution, as described in Section 4.

$$F_{\mathrm{DEP}} = 2\pi\varepsilon_m a^3 K \nabla E_0^2, \qquad K = \frac{\varepsilon_p - \varepsilon_m}{\varepsilon_p + \varepsilon_m}. \tag{6}$$

One successful example of a strong DEP response to light was the "optoelectronic tweezers" demonstrated by Chiou *et al.* [27]. A colloidal suspension between a photoconductive layer of Si and a conductive layer of indium tin oxide (ITO) was biased with an AC signal. Incident light on the Si layer increased the conductivity and created a localized (nonuniform) electric field in the colloid layer to induce particle trapping. The mechanical response in this type of system results from multiple forces in addition to DEP, making it difficult to accurately model. With the electrothermal force, fluid heats up in the presence of the electric field and motion is induced in the fluid due to the temperature gradient. This microvortex brings particles in toward the nonuniformity [28,29]. The electroosmosis force is due to the charged electrode surface creating an electric double layer in the otherwise neutral fluid. With the tangential electric field component and the charged double layer, electrophoresis induces a fluidic motion toward the charged area [28,29].

Figure 10 shows two configurations where such electrically enhanced optical trapping can meet the requirements of a reactive solar concentrator. In Fig. 10(a), a photoconductive layer is connected to an applied AC voltage source, following the form of previously demonstrated optoelectronic trapping systems. This requires an external power supply. In Fig. 10(b), a thin organic photovoltaic layer is placed in between the fluid and the waveguide. As the sunlight hits this PV layer, a small percentage will be absorbed and create an induced local electric field across the colloidal suspension, and a strong index response. The PV layer does not represent a significant optical loss: unlike the materials used in a PV panel, the system is not connected to a load and does not generate a sustained photocurrent, making it possible to achieve a local voltage with very low absorption, or absorption only in a spectral band which would otherwise be unused. With a small gap, a small voltage can still generate a large electric field.

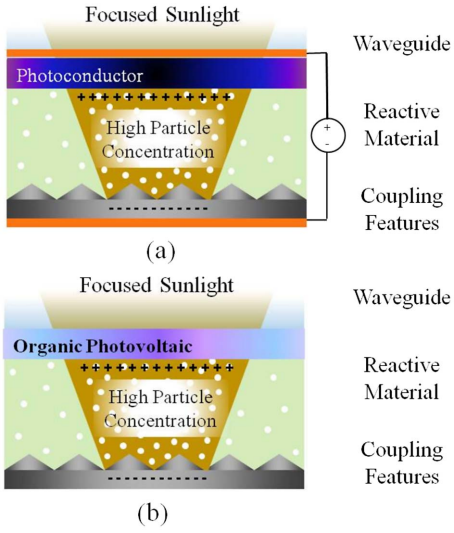

Fig. 10. (Color online) Optically induced DEP trapping: the focused sunlight induces a local change in the electric field through an externally biased photoconductor (a) or an organic photovoltaic (b), pulling in high-index particles and locally increasing the index of refraction.

4. Materials Characterization

With a mechanism to provide the needed change in index, our next step was to identify potential materials and characterize the response using available materials. Bulk crystalline titanium dioxide (TiO_2) (rutile) has an index of refraction of 2.5, providing the potential for a large index difference relative to solvents. The high specific gravity of TiO_2 and the potential for particle aggregation (clumping) can make it difficult to obtain a stable suspension, but research at the University of Arizona has demonstrated long-term stable colloids containing UV passivated TiO_2 nanoparticles [30]. They have successfully created a long-term stable suspension of 13.1% by volume 5 nm TiO_2 particles in ethanol [31]. This makes TiO_2 the most promising material candidate to achieve the index response needed. Perfluorocompounds such as as FC-70 (perfluorotriamylamine) are both low-index and high density, representing the ideal medium. However, as this suspension was not readily available, we conducted proof of concept tests using aqueous polystyrene, a common test material for nanofluidic systems. The difference in index of refraction between water and polystyrene is 0.26, and packing statistics limit the maximum percentage of polystyrene to 76%, limiting the achievable index response to much less than the needed change of 0.3.

Initial experimental results demonstrate DEP-induced particle concentration in order to locally increase the index of refraction of a colloid. Our experimental setup used patterned ITO electrodes on glass slides to induce a nonuniform electric field as shown in Fig. 11. The test colloid was placed between the patterned ITO and a solid ITO coated slides and held in place by a 25 um thick washer. This geometry mimics the nonuniform electrical field that could be

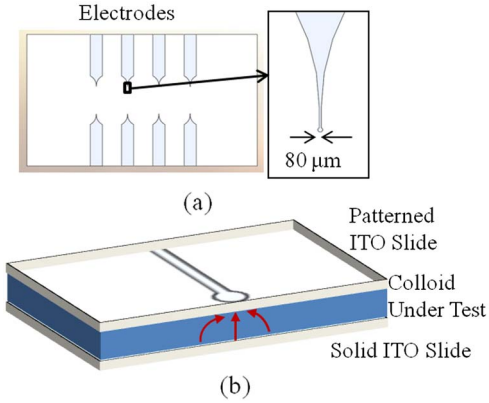

Fig. 11. (Color online) Patterned ITO electrodes (a) are used in the system (b) to see the effect of a nonuniform electric field on a colloid.

produced by the designs shown in Fig. 10. Index response was measured by a Mach–Zehnder interferometer, generating the interferograms shown in Fig. 12. The bias was applied across the electrodes for 60 seconds, and the system was allowed to rest for 10 minutes between tests to allow the particles to disperse and the sample to return to thermal equilibrium. After measuring the number of fringe shifts seen in the area of nonuniformity, the total change in index can be calculated by $\Delta n = (\lambda/d) * s$, where λ is the wavelength, d is the depth of the fluid, and s is the number of fringe shifts.

A 10% by volume aqueous suspension of 60 nm polystyrene particles (Thermo Scientific 5000 Series) was tested with both a DC signal and a 60 Hz square wave signal. We found that while a DC signal induced a response, nonuniform space charge effects made data unrepeatable. The results of initial characterization, including those shown in Fig. 13, used only AC fields. The shift occurred within about 45 seconds, making the speed of this reaction appropriate for use in response to moving sunlight. The average change in index seen at 2 volts rms was 0.033, raising the index of refraction from 1.356 to 1.389. This indicates an increase of more than double the local concentration by volume from 10% to 23%. Tests performed with pure deionized water showed no response, indicating that the demonstrated effect is from concentrated particles and not a thermal change. Tests with lower concentrations of polystyrene showed a smaller response consistent with the same relative increase in concentration. However, with less than one full fringe shift, these materials changes could not be accurately characterized.

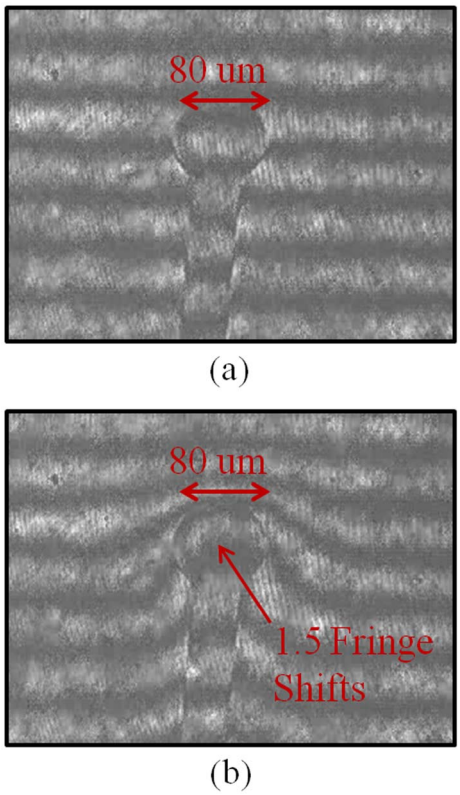

Fig. 12. (Color online) Interferograms before (a) and after (b) 60 seconds of 60 Hz 2 volt rms square wave. The shift in the fringe pattern indicates a change in the index of refraction.

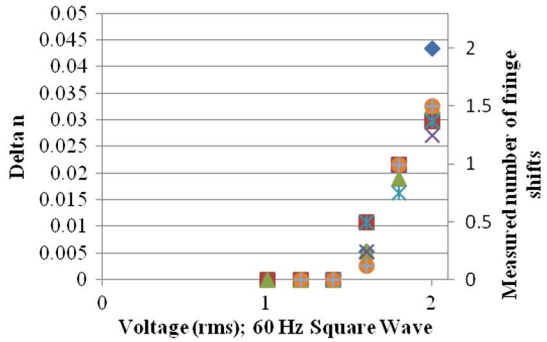

Fig. 13. (Color online) Number of fringe shifts measured and change in index of refraction calculated for varying power 60 Hz square wave.

These tests demonstrate the use of DEP trapping to change the local index of refraction of a material and show promise in terms of meeting the temporal response and reversibility. A response eight times larger is needed for efficient reactive tracking of a planar micro-optic solar concentrator, and so future work will involve tests with TiO_2 suspensions. A stable suspension of TiO_2 particles in a low-index, high density fluid such as FC-70 would have a Clausius-Mosotti factor 3.4 times larger than aqueous polystyrene. The same increase in particle concentration from 10% to 23% would result in a change of index of refraction from 1.400 to 1.542. The target Δn of 0.3 could be obtained at the same relative increase in concentration by volume by starting at 19% and increasing to 44% ($n = 1.50$ to 1.80). The question of maximum practical particle density has not been resolved, so it may be preferable to start from a lower density and increase by a larger factor.

5. Conclusions/Future Work

In this paper we have presented the concept of reactive solar tracking, using an intrinsic materials response to enable efficient high-concentration systems without precise mechanical tracking and without violating étendue limits. Previous work on planar micro-optic solar concentration demonstrated a high-efficiency concentrator compatible with inexpensive roll-to-roll processing but which would still require precise two-axis mechanical tracking comparable to conventional high-concentration optics. Here we show that introducing a material capable of a localized increase in refractive index in response to focused sunlight enables efficient coupling of sunlight from a range of angles into the output waveguide. We found that a 128× geometric concentrator designed with such a material can have 85% optical efficiency for on-axis light, and accept 83% of total annual energy incident on a planar collector mounted on a low-precision one-axis tracker.

For this reactive concentrator design, the index of refraction of the illuminated reactive material must

increase by a substantial 0.3, and react quickly enough to track with sunlight moving at 40 um per minute. We identified a promising material system to achieve this using optically induced concentration of high-index particles in a low-index suspension. Calculations for direct optical trapping from microlens-focused sunlight show insufficient force to achieve the required index response. However, optically induced DEP can provide a stronger trapping force for the same optical input, and our calculations show the required index change can be achieved using a suspension of high-index TiO_2 nanoparticles in a low-index fluid. We presented initial experimental work with aqueous polystyrene, demonstrating a 0.033 local change of index in response to a 2 V rms 60 Hz square wave signal, and indicating that the required index response is achievable with an optimized material system. We conclude that the reactive waveguide cladding is a promising direction for high-concentration PV systems with significantly reduced requirements for mechanical tracking.

The authors would like to thank Robert Norwood and Palash Gangopadhyay of the University of Arizona for materials, information, and preparation.

This research was made possible by support from the National Science Foundation (NSF) under SGER award #0844274 and from the California Energy Commission as part of the California Solar Energy Collaborative.

References

1. S. Kurtz, "Opportunities and Challenges for Development of a Mature Concentrating Photovoltaic Power Industry," (NREL, 2010).
2. H. Ullal, R. Mitchell, B. Keyes, K. VanSant, B. von Roedern, M. Symko-Davies, and V. Kane, "Progress of the photovoltaic technology incubator project towards an enhanced U. S. manufacturing base," presented at the *37th IEEE Photovoltaic Specialists Conference (PVSC 37)*, Seattle (19–24 June 2011).
3. J. W. Garland, T. Biegala, M. Carmody, C. Gilmore, and S. Sivananthan, "Next-generation multijunction solar cells: The promise of II–VI materials," J. Appl. Phys. **109**, 102423 (2011).
4. W. T. Welford and R. Winston, *The Optics of Non-imaging Concentrators: Light and Solar Energy* (Academic, 1978).
5. W. H. Weber and J. Lambe, "Luminescent greenhouse collector for solar radiation," Appl. Opt. **15**, 2299–2300 (1976).
6. M. J. Currie, J. K. Mapel, T. D. Heidel, S. Goffri, and M. A. Baldo, "High-efficiency organic solar concentrators for photovoltaics," Science **321**, 226–228 (2008).
7. G. V. Shcherbatyuk, R. H. Inman, C. Wang, R. Winston, and S. Ghosh, "Viability of using near infrared PbS quantum dots as active materials in luminescent solar concentrators," Appl. Phys. Lett. **96**, 191901 (2010).
8. J. H. Karp, E. J. Tremblay, and J. E. Ford, "Planar micro-optic solar concentrator," Opt. Express **18**, 137–144 (2010).
9. J. H. Karp, E. J. Tremblay, J. M. Hallas, and J. E. Ford, "Orthogonal and secondary concentration in planar micro-optic solar collectors," Opt. Express **19**, A673–A685 (2011).
10. C. Y. Chang, S. Y. Yang, and J. L. Sheh, "A roller embossing process for rapid fabrication of microlens arrays on glass substrates," Microsyst. Technol. **12**, 754–759 (2006).
11. S. H. Ahn and L. J. Guo, "High-speed roll-to-roll nanoimprint lithography on flexible plastic substrates," Adv. Mater. **20**, 2044–2049 (2008).
12. B. L. Unger, G. R. Schmidt, and D. T. Moore, "Dimpled planar lightguide solar concentrators," in *OSA International Optical Design Conference* (Optical Society of America, 2010).
13. J. P. Morgan, "Light-guide solar panel and method of fabrication thereof," Morgan Solar, Inc. World Intellectual Property Organization, WO 2008/131561, 11 June 2008.
14. S. Ghosh and D. S. Schultz, "Solar energy concentrator," Banyan Energy, Inc., U.S. Patent 7,672,549B2 (2 March 2010).
15. J. M. Hallas, J. H. Karp, E. J. Tremblay, and J. E. Ford, "Lateral translation micro-tracking of planar micro-optic solar concentrator," Proc. SPIE **7769**, 776904 (2010).
16. F. Duerr, Y. Meuret, and H. Thienpont, "Tracking integration in concentrating photovoltaics using laterally moving optics," Opt. Express **19**, A207–A218 (2011).
17. P. H. Schmaelzle and G. L. Whiting, "Lower critical solution temperature (LCST) polymers as a self adaptive alternative to mechanical tracking for solar energy harvesting devices," presented at the MRS Fall Meeting, Boston (29 November–3 December 2010).
18. A. Rabl, *Active Solar Collectors and Their Applications* (Oxford University, 1985).
19. A. Ashkin, J. M. Dziedzic, and P. W. Smith, "Continuous-wave self-focusing and self-trapping of light in artificial Kerr media," Opt. Lett. **7**, 276–278 (1982).
20. V. E. Yashin, S. A. Chizhov, R. L. Sabirov, T. V. Starchikova, N. V. Vysotina, N. N. Rozanov, V. E. Semenov, V. A. Smirnov, and S. V. Fedorov, "Formation of soliton-like light beams in an aqueous suspension of polystyrene particles," Opt. Spectrosc. **98**, 466–469 (2005).
21. R. Gordon and J. T. Blakely, "Particle-optical self-trapping," Phys. Rev. A **75**, 8–11 (2007).
22. M. Kuzyk, *Polymer Fiber Optics* (CRC/Taylor & Francis, 2007).
23. W. M. Lee, R. El-Ganainy, D. N. Christodoulides, K. Dholakia, and E. M. Wright, "Nonlinear optical response of colloidal suspensions," Opt. Express **17**, 10277–10289 (2009).
24. H. Pohl, "The motion and precipitation of suspensoids in divergent electric fields," J. Appl. Phys. **22**, 869–871 (1951).
25. T. Jones, *Electromechanics of Particles* (Cambridge University, 1995).
26. D. Chen, H. Du, and C. Y. Tay, "Rapid concentration of nanoparticles with DC dielectrophoresis in focused electric fields," Nanoscale Res. Lett. **5**, 55–60 (2010).
27. P. Y. Chiou, A. T. Ohta, and M. C. Wu, "Massively parallel manipulation of single cells and microparticles using optical images," Nature **436**, 370–372 (2005).
28. S. J. Williams, A. Kumar, and S. T. Wereley, "Electrokinetic patterning of colloidal particles with optical landscapes," Lab Chip **8**, 1879–1882 (2008).
29. J. K. Valley, A. Jamshidi, A. T. Ohta, H.-Y. Hsu, and M. C. Wu, "Operational regimes and physics present in optoelectronic tweezers," J. Microelectromech. Syst. **17**, 342–350 (2008).
30. R. Himmelhuber, P. Gangopadhyay, R. A. Norwood, D. A. Loy, and N. Peyghambarian, "Titanium oxide sol-gel films with tunable refractive index," Opt. Mat. Express **1**, 252–258 (2011).
31. R. A. Norwood, Department of Optical Sciences, University of Arizona, (personal communication, 2010).